



## Transition in plane parallel shear flows heated internally

Masato Nagata<sup>a</sup>, Sotos Generalis<sup>b</sup>

<sup>a</sup> Department of Aeronautics and Astronautics, Graduate School of Engineering, Kyoto University, Kyoto 606-8501, Japan

<sup>b</sup> School of Engineering and Applied Sciences, Division of Chemical Engineering and Applied Chemistry, Aston University, UK

Received 11 August 2003; accepted after revision 21 October 2003

Presented by Évariste Sanchez-Palencia

### Abstract

The stability of internally heated inclined plane parallel shear flows is examined numerically for the case of finite value of the Prandtl number,  $Pr$ . The transition in a vertical channel has already been studied for  $0 \leq Pr \leq 100$  with or without the application of an external pressure gradient, where the secondary flow takes the form of travelling waves (TWs) that are spanwise-independent (see works of Nagata and Generalis). In this work, in contrast to work already reported (J. Heat Trans. T. ASME 124 (2002) 635–642), we examine transition where the secondary flow takes the form of longitudinal rolls (LRs), which are independent of the streamwise direction, for  $Pr = 7$  and for a specific value of the angle of inclination of the fluid layer without the application of an external pressure gradient. We find possible bifurcation points of the secondary flow by performing a linear stability analysis that determines the neutral curve, where the basic flow, which can have two inflection points, loses stability. The linear stability of the secondary flow against three-dimensional perturbations is also examined numerically for the same value of the angle of inclination by employing Floquet theory. We identify possible bifurcation points for the tertiary flow and show that the bifurcation can be either monotone or oscillatory. **To cite this article: M. Nagata, S. Generalis, C. R. Mecanique 332 (2004).**

© 2003 Académie des sciences. Published by Elsevier SAS. All rights reserved.

### Résumé

**Transition dans des écoulements cisailés parallèles chauffés intérieurement.** On présente une étude numérique de la stabilité d'écoulements parallèles cisailés plans, chauffés intérieurement, dans le cas du nombre de Prandtl  $Pr$  fini. On a déjà étudié la transition dans un conduit vertical pour  $0 \leq Pr \leq 100$  avec ou sans application d'un gradient de pression extérieure, quand l'écoulement secondaire prend la forme d'ondes progressives (TW), indépendantes de l'envergure de l'écoulement (voir les publications de Nagata et Generalis). Dans le travail présent, contrairement aux résultats déjà rapportés (J. Heat Trans. T. ASME 124 (2002) 635–642), on examine la transition pendant laquelle l'écoulement secondaire prend la forme des rouleaux longitudinaux (LRs), indépendants de la direction du flux, pour  $Pr = 7$  et pour une valeur spécifique de l'angle d'inclinaison de la couche fluide, sans application du gradient de pression extérieure. Nous trouvons les points de bifurcation possibles de l'écoulement secondaire en effectuant une analyse de stabilité linéaire permettant de déterminer la courbe neutre, sur laquelle l'écoulement de base peut présenter deux points d'inflexion, perdant sa stabilité. La stabilité linéaire de l'écoulement secondaire par rapport aux perturbations tri-dimensionnelles a été examinée également pour une valeur constante de l'angle d'inclinaison, à l'aide de la théorie de Floquet. On identifie les points de bifurcation possibles pour l'écoulement tertiaire ; on montre aussi que

E-mail addresses: [nagata@kuaero.kyoto-u.ac.jp](mailto:nagata@kuaero.kyoto-u.ac.jp) (M. Nagata), [s.c.generalis@aston.ac.uk](mailto:s.c.generalis@aston.ac.uk) (S. Generalis).

cette bifurcation peut être soit monotone, soit oscillatoire. *Pour citer cet article* : M. Nagata, S. Generalis, C. R. Mecanique 332 (2004).

© 2003 Académie des sciences. Published by Elsevier SAS. All rights reserved.

*Keywords*: Heat transfer; Shear flow; Internal heat; Secondary instability; Transition; Floquet theory

*Mots-clés* : Transferts thermiques ; Écoulement cisaillé ; Chaleur interne ; Instabilité secondaire ; Théorie de Floquet

## 1. Introduction

The objective of our study is to provide significant insights into the identification of the mechanisms for instability and transition from laminar to turbulent state in flows with homogeneously distributed heat source. To this end we consider incompressible viscous flow in an inclined channel with an internal heat source. Such a heat source may be produced, for example, through a mechanism in the nuclear fusion industry, where liquid sodium is used to cool the hot plasma, and therefore due to its nuclear safety issues the problem of internally heated flows has recently attracted attention [4] (and references therein). In the present study we consider a Cartesian coordinate system positioned in the midplane of the fluid layer of width  $2d$  bounded between two parallel plates of infinite extent with  $x, y, z$  the streamwise, spanwise and horizontal directions with unit vectors  $\hat{\mathbf{i}}, \hat{\mathbf{j}}, \hat{\mathbf{k}}$  respectively. The two plates are maintained at constant temperature  $T = T_0$  (see Fig. 1). We apply the Boussinesq approximation and use  $d, d^2/\nu$  and  $qd^2/2\kappa Gr$ , where  $Gr = g\delta qd^5/2\kappa\nu^2$  is the Grashof number (the non-dimensional parameter that provides the strength of the internal heat source), as the units of length, time and temperature respectively [2], to obtain the following non-dimensional Navier–Stokes equations for the velocity vector  $\mathbf{u}$  and temperature variation  $T$  from the environment ( $q$  is the volume strength of the heat source that generates the basic flow,  $\kappa$  is the thermal diffusivity,  $\delta$  is the coefficient of thermal expansion,  $\nu$  is the kinematic viscosity,  $\gamma$  is the angle of inclination of the fluid layer and  $g$  is the acceleration due to gravity):

$$\frac{\partial}{\partial t} \mathbf{u} + \mathbf{u} \cdot \nabla \mathbf{u} = 2R + (\hat{\mathbf{i}} \sin(\gamma) + \hat{\mathbf{k}} \cos(\gamma))T + \nabla^2 \mathbf{u} \quad (1)$$

$$\frac{\partial}{\partial t} T + \mathbf{u} \cdot \nabla T = Pr^{-1}(\nabla^2 T + 2Gr) \quad (2)$$

$$\nabla \cdot \mathbf{u} = 0 \quad (3)$$

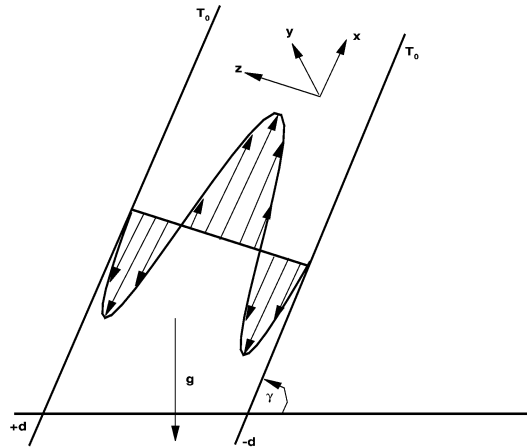


Fig. 1. Geometrical configuration exhibiting the basic flow profile with two inflection points in an inclined fluid layer heated internally.

where  $Pr = \nu/\kappa$  is the Prandtl number and  $R = U_{\max}d/\nu = -d^3\nabla\pi/2\nu^2\rho$  is the Reynolds number that measures the strength of the applied pressure gradient. Here  $U_{\max}$  is the maximum laminar velocity for pure Poiseuille flow [1] and  $\pi$  is the pressure. The assumption of the Boussinesq approximation ensures that the density  $\rho$  is regarded as constant except for the gravity term. Terms that can be written as gradients, have been combined into the expression for  $R$ . The boundary conditions are

$$\mathbf{u}(z = \pm 1) = T(z = \pm 1) = 0 \quad (4)$$

The basic solution of Eqs. (1)–(3) consists of a basic velocity profile  $\mathbf{u}_0 = U_0(z)\hat{\mathbf{i}}$  and a basic temperature distribution  $T_0(z)$  of the form [1,2]

$$U_0(z) = ((Gr \sin(\gamma)/12)(z^4 - 6z^2 + 5) + R(1 - z^2)) \quad (5)$$

$$T_0(z) = Gr(1 - z^2) \quad (6)$$

The basic velocity profile of Eq. (5) has two inflection points if the Reynolds number satisfies  $-Gr/2 \leq R \leq 0$  and so we can expect the steady basic state to be linearly unstable, although the Rayleigh instability criteria are applicable only to inviscid cases. The effects of an applied pressure gradient on the transition of internally heated flow were considered in [1]. In the present work we assume a vanishing value of  $R$  ( $R = 0$ ). In the following section we derive the equations of disturbances and in Section 3 we investigate the linear stability of our basic steady state (Eqs. (5), (6)) numerically using the method of [1,2] for  $Pr = 7$ .

## 2. Mathematical model

In order to describe secondary solutions that bifurcate from the basic flow we follow [2] and we separate the velocity field deviations  $\hat{\mathbf{u}}$  (from the basic flow of Eq. (5)) and temperature deviations,  $\theta$  (from the basic flow of Eq. (6)) into an average part (over the  $x$  and  $y$  coordinates)  $\check{U}$ ,  $\check{T}$ , (see [2]), and a fluctuating part  $\check{\mathbf{u}}$ ,  $\check{\theta}$  (with a vanishing average over the  $x$  and  $y$  coordinates):

$$\hat{\mathbf{u}} = \check{U} + \check{\mathbf{u}} \quad (7)$$

$$\theta = \check{T} + \check{\theta} \quad (8)$$

where

$$\check{\mathbf{u}} = \delta\phi + \varepsilon\psi = \nabla \times (\nabla \times \hat{\mathbf{k}}\phi) + \nabla \times (\hat{\mathbf{k}}\psi) \quad (9)$$

with the total mean flow and the total mean temperature given by

$$\hat{U} = U_0 + \check{U} \quad (10)$$

$$\hat{T} = T_0 + \check{T} \quad (11)$$

In Eq. (9)  $\phi$ ,  $\psi$  refers to the poloidal and toroidal part of the velocity fluctuations respectively [1–3], satisfying  $\overline{\phi} = \overline{\psi} = 0$ , where the overbar denotes the  $x - y$  average [1]. It is worth pointing out that the incompressibility condition is satisfied automatically for the decomposition of Eq. (9) of the velocity field and can therefore be eliminated from the rest of the analysis. By applying the operators  $\delta \cdot$  and  $\varepsilon \cdot$  (for simplicity of notation we drop the  $\sim$  from the temperature fluctuations  $\theta$  hereafter) we obtain the following equations for the poloidal and toroidal parts of the velocity fluctuations:

$$\begin{aligned} \frac{\partial}{\partial t} \nabla^2 \Delta_2 \phi - \nabla^4 \Delta_2 \phi + \hat{U} \partial_x \nabla_2 \Delta_2 \phi \\ = \partial_z^2 \hat{U} \Delta_2 \partial_x \phi + \sin(\gamma) \partial_x \partial_z \theta - \cos(\gamma) \Delta_2 \theta - \delta \cdot \{(\delta\phi + \varepsilon\psi) \cdot \nabla(\delta\phi + \varepsilon\psi)\} \end{aligned} \quad (12)$$

$$\frac{\partial}{\partial t} \Delta_2 \psi - \sin(\gamma) \partial_y \theta - \nabla^2 \Delta_2 \psi = \partial_z \hat{U} \Delta_2 \partial_y \phi - \hat{U} \partial_x \Delta_2 \psi - \varepsilon \cdot \{(\delta\phi + \varepsilon\psi) \cdot \nabla(\delta\phi + \varepsilon\psi)\} \quad (13)$$

We can now rewrite the temperature equation as

$$\frac{\partial}{\partial t}\theta = -2Gr(\mathbf{r} \cdot \hat{\mathbf{k}})\Delta_2\phi + \Delta_2\phi\partial_z\check{T} - \widehat{U}\partial_x\theta + Pr^{-1}\nabla^2\theta - (\delta\phi + \varepsilon\psi) \cdot \nabla\theta \quad (14)$$

where  $\Delta_2 \equiv \partial_x^2 + \partial_y^2$  is the planform Laplacian. The mean flow and temperature,  $\check{U}(z, t)$  and  $\check{T}(z, t)$ , satisfy

$$\partial_z^2\check{U} + \sin(\gamma)\check{T} + \partial_z\overline{\Delta_2\phi(\partial_x\partial_z\phi + \partial_y\psi)} = \partial_t\check{U} \quad (15)$$

$$\partial_z^2\check{T} + Pr\partial_z\overline{\Delta_2\phi\theta} = Pr\partial_t\check{T} \quad (16)$$

The no-slip and fixed temperature conditions on the plates for  $\phi$ ,  $\psi$ ,  $\theta$ ,  $\check{U}$  and  $\check{T}$  are

$$\phi = \frac{\partial\phi}{\partial z} = \psi = \theta = \check{U} = \check{T} = 0 \quad \text{at } z = \pm 1 \quad (17)$$

In the next section the linear stability of the basic flow and temperature profiles of Eqs. (5), (6) is examined with respect to infinitesimal perturbations.

### 3. Linear stability analysis – Longitudinal Roll (LR) type disturbances

In order to study the linear stability characteristics of the LR type disturbances we ignore the nonlinear terms of Eqs. (12)–(14), the mean flow and mean temperature of Eqs. (15), (16) and we set  $\partial_x = 0$ , thus considering the stability of the parallel flow in the spanwise direction [2]. Additionally we expand the temperature fluctuations and the poloidal and toroidal parts of the velocity fluctuations in terms of orthogonal functions [2]

$$\phi = \sum_{n=-N, n \neq 0}^N \sum_{l=0}^L a_{nl} \exp\{in\beta y\}(1-z^2)^2 T_l \quad (18)$$

$$\psi = \sum_{n=-N, n \neq 0}^N \sum_{l=0}^L b_{nl} \exp\{in\beta y\}(1-z^2) T_l \quad (19)$$

$$\theta = \sum_{n=-N, n \neq 0}^N \sum_{l=0}^L c_{nl} \exp\{in\beta y\}(1-z^2) T_l \quad (20)$$

The factors  $(1-z^2)^2$  and  $1-z^2$  in Eqs. (18)–(20) are necessary in view of the boundary conditions (Eq. (17)),  $a_{nl}$ ,  $b_{nl}$ , and  $c_{nl}$  are unknown complex coefficients,  $\beta$  is the wave number of the LR disturbance and  $T_l$  is the  $l$ -th order Chebyshev polynomial. Similar expansions for the fluctuations are employed when considering travelling wave (TW) disturbances with wave number  $\alpha$  in the streamwise direction (and  $\beta = 0$ ) with the phase velocity of the TW disturbances as an additional parameter [1]. The stability of the streamwise (TW) disturbances was examined in [2]. For the linear analysis of this section only one mode in the spanwise direction is retained. In order to study the linear stability characteristics of the LR disturbances we therefore write:

$$\phi = \sum_{l=0}^L a_l \exp\{i\beta y + \sigma t\}(1-z^2)^2 T_l$$

$$\psi = \sum_{l=0}^L b_l \exp\{i\beta y + \sigma t\}(1-z^2) T_l$$

$$\theta = \sum_{l=0}^L c_l \exp\{i\beta y + \sigma t\}(1-z^2) T_l$$

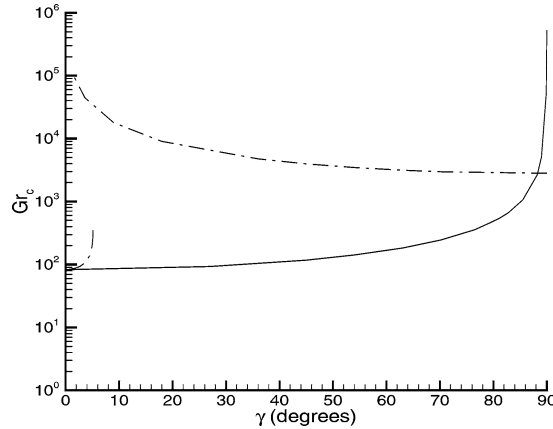


Fig. 2. Critical Grashof number as a function of the angle of inclination for LR $s$  ( $\alpha = 0$ , continuous curve). The dash-dotted, disconnected, curves represent the critical Grashof number for TW $s$  ( $\beta = 0$ ) [2]. The upper dash-dotted curve merges with the lower dash-dotted curve at  $\gamma \approx 0.9^\circ$ .  $Pr = 7$ ,  $R = 0$ .

where the real part of the complex  $\sigma$ ,  $\sigma_r$ , defines the rate of damping or amplification of the perturbations. We then employ the Chebyshev collocation point method of [1,2] to obtain a generalized algebraic eigenvalue problem:

$$A\mathbf{x} = \sigma B\mathbf{x} \tag{21}$$

where  $\mathbf{x} = (a_{10}, \dots, a_{1L}, b_{10}, \dots, b_{1L}, c_{10}, \dots, c_{1L})^T$  with  $A, B$  complex matrices. The QZ method was utilized to solve the eigenvalue problem of Eq. (21) with the use of the NAG subroutine F02GJF. In order to achieve numerical accuracy of the results a high enough truncation number must be chosen. It was found that for the case  $Pr = 7$ ,  $L \geq 13$  was satisfactory. We note here that for all values of  $\gamma$  examined the imaginary part of the leading eigenvalue  $\sigma_1$  for LR disturbances is always zero [2]. In Fig. 2 the critical Grashof numbers as functions of the angle of inclination are given. In the same figure we have also superimposed the curve that provides the critical Grashof number for TW disturbances [2]. The reason for the apparent discontinuity at  $\gamma \approx 0.9^\circ$  of the dash-dotted curve (TW disturbances) is given in [2]. As is evident from Fig. 2 our basic flow becomes unstable to TW disturbances for much lower  $Gr$  values than LR perturbations for values of  $\gamma \approx 90^\circ$ , while for almost all other values of  $\gamma$  it becomes unstable to LR disturbances. In the horizontal configuration, however, both LR and TW disturbances share the same value of the critical Grashof number. In the following section we study the nonlinear secondary LR $s$  that bifurcate from the neutral curves of Fig. 2 for  $\gamma = 60^\circ$ .

#### 4. Secondary longitudinal rolls

##### 4.1. Numerical method

In this section we calculate the two-dimensional nonlinear equilibrium solutions that are created at the neutral curves for  $\gamma = 60^\circ$ , as predicted by the linear analysis discussed in the previous section (see Fig. 2). Here we set  $\partial_x = 0$  and additionally retain the non-linear terms of Eqs. (12)–(14) and the mean flow and mean temperature of Eqs. (15), (16). Finally we note that Eqs. (12)–(16) are subject to the homogeneous boundary conditions of Eq. (17). For the mean flow and mean temperature distortions of Eqs. (15), (16) we write:

$$\check{U} = \sum_{l=0}^L C_l (1 - z^2) T_l \tag{22}$$

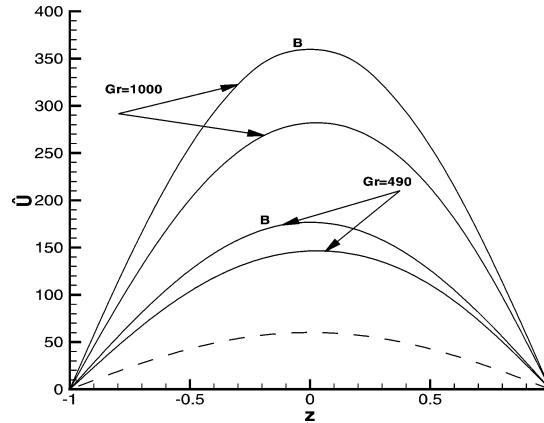


Fig. 3. Total mean flow ( $\check{U}$ ) profile for a fixed wave number  $\beta = 2.0$  and for various Grashof numbers as indicated. Curves marked with B represent the contributions of Eq. (5). The dashed curve represents the basic flow contribution for  $Gr_c = 166.62919$ . Here  $Pr = 7$ ,  $R = 0$ ,  $\gamma = 60^\circ$ .

$$\check{T} = \sum_{l=0}^L D_l (1 - z^2) T_l \quad (23)$$

The factor  $1 - z^2$  has been introduced in the expansions of  $\check{U}$  and  $\check{T}$ , so that the conditions of Eq. (17) are satisfied. When Eqs. (18)–(20) and Eqs. (22), (23) are substituted in Eqs. (12)–(16) the non-linear secondary equilibrium solutions are obtained with the aid of the Chebyshev collocation point method and the Newton–Raphson iterative method outlined in [2], for some high enough truncation parameters  $N$ ,  $L$ . Supercritical LR solutions have been obtained for a variety of values of the Grashof number, spanwise wave number and angle of inclination, but in this work we restrict our attention to the case where  $Pr = 7$  and  $\gamma = 60^\circ$ .

#### 4.2. Results

Well-converged supercritical secondary solutions have been obtained for  $L \geq 13$ ,  $N = 5$ . These two parameter values were therefore retained for this work and for consistency with the linear analysis of the previous section. In Fig. 3 we show the total mean supercritical flow of Eq. (10) plotted against the channel width, for the nonlinear equilibrium state characterized by  $\beta = 2.0$  for various values of  $Gr$  and for the case  $Pr = 7$  and  $\gamma = 60^\circ$ . A more detailed analysis of the characteristics of the secondary flow for  $\gamma = 60^\circ$  as well as for  $0^\circ \leq \gamma \leq 89^\circ$ , will be presented separately. In the following section we examine the stability of the secondary solutions obtained in this section.

### 5. Stability of secondary LRs

We now study the linear stability of the secondary flow of the previous section, in order to identify possible bifurcation points for the tertiary flow for  $\gamma = 60^\circ$ . We superimpose three-dimensional (solenoidal) infinitesimal disturbances on the secondary flow  $\widehat{U}\mathbf{i} + \check{\mathbf{u}}$  and temperature  $\widehat{T} + \theta$  in the form

$$\check{\mathbf{u}} = \delta\check{\phi} + \varepsilon\check{\psi}, \quad \check{\theta} = \check{\theta} \quad (24)$$

and we seek to numerically evaluate their growth rates  $\sigma$ . Disturbances with  $\sigma_r < 0$  will indicate a stable secondary solution, while for  $\sigma_r = 0$  we have neutral stability and possibility of bifurcation for the tertiary flow. Possible

bifurcation points of three-dimensional solutions (that bifurcate from the secondary neutral curves) are computed via linear secondary stability theory [1,2], as described briefly in the following section.

### 5.1. Numerical method

Applying the Floquet theory, we set, [1,2]:

$$\tilde{\phi} = \sum_{n=-N}^N \sum_{l=0}^L \tilde{a}_{nl} \exp\{in\beta y + i(dx + by) + \sigma t\} \times (1 - z^2)^2 T_l(z) \tag{25}$$

$$\tilde{\psi} = \sum_{n=-N}^N \sum_{l=0}^L \tilde{b}_{nl} \exp\{in\beta y + i(dx + by) + \sigma t\} \times (1 - z^2) T_l(z) \tag{26}$$

$$\tilde{\theta} = \sum_{n=-N}^N \sum_{l=0}^L \tilde{c}_{nl} \exp\{in\beta y + i(dx + by) + \sigma t\} \times (1 - z^2) T_l(z) \tag{27}$$

for the complex disturbances  $\{\tilde{\phi}, \tilde{\psi}, \tilde{\theta}\}$  that satisfy the boundary conditions:

$$\tilde{\phi} = \frac{\partial \tilde{\phi}}{\partial z} = \tilde{\psi} = \tilde{\theta} = 0 \quad \text{at } z = \pm 1 \tag{28}$$

In order to derive the corresponding equations for the disturbance field  $\{\tilde{\phi}, \tilde{\psi}, \tilde{\theta}\}$ , we follow [2], and we replace  $\phi, \psi, \theta$  in Eqs. (12)–(14) by  $\phi + \tilde{\phi}, \psi + \tilde{\psi}, \theta + \tilde{\theta}$ , respectively and we subtract the equations for the steady solution  $\phi, \psi, \theta$ . As the value of  $d^2 + b^2$  will be assumed to be different from zero for the rest of the analysis, there are no contributions to the mean flow and temperature. Following the method outlined in [1,2] the following generalized algebraic eigenvalue problem results:

$$A\tilde{x} = \sigma B\tilde{x} \tag{29}$$

in the unknown complex variables  $\{\tilde{a}_{nl}, \tilde{b}_{nl}, \tilde{c}_{nl}\}$  represented by  $\tilde{x}$ . The  $3(L + 1)(2N + 1)$  matrices  $A, B$  are functions of the real parameters  $d, b, Gr, Pr, \gamma$ , the wave number  $\beta$  and the amplitudes of the steady state solution  $\{a_{nl}, b_{nl}, c_{nl}, C_l, D_l\}$ . Eqs. (29) are solved with the use of the NAG subroutine F02GJF. The same truncation level was used in this section as that retained for the steady solutions of the previous section. The real part  $\sigma_{1r}$  of the leading eigenvalue  $\sigma_1$  determines the rate of damping or amplification of the disturbance. The stability boundary is obtained by the condition  $\sigma_{1r} = 0$ . Finally we note that in all cases examined the symmetry relations  $\sigma_{1r}(b, d) = \sigma_{1r}(b, \pm d) = \sigma_{1r}(\pm b, d)$  were always confirmed. The results of our studies for the case  $\gamma = 60^\circ$  are briefly described below.

### 5.2. Results

In Fig. 4 we present the stability range of LRs for the case  $Pr = 7$ , and  $R = 0$ . As can be seen from Fig. 4 the boundary is formed by Eckhaus and Hopf bifurcation curves. The term Hopf bifurcation usually refers to the crossing of the imaginary axis by two complex eigenvalues. In the context of the present work, however, the term Hopf bifurcation is used when only one complex eigenvalue is active in the bifurcation process. This terminology has been used before and has been accepted in the literature [1–3,5]. For the Eckhaus curve, which bounds the area of the stable LRs towards larger and lower wave numbers,  $d = 0$ . Several values of the Grashof number were studied and the maximum real part of the leading eigenvalue  $\sigma_1$  was evaluated. The value of  $Gr$ , which determines the boundary of the curve, was calculated by interpolation. In order to determine such boundaries for a given value of the Grashof number that characterizes a secondary solution, we determine the eigenvalue of Eq. (29) as a function of the parameters  $b, d$ . We examined a variety of combinations of the relevant parameters, where a large

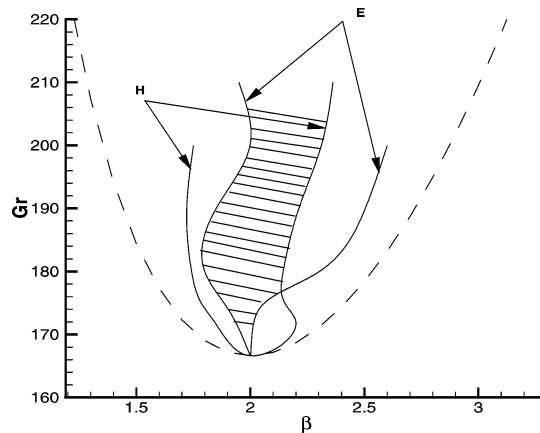


Fig. 4. Instability boundaries of secondary LR for the case  $Pr = 7$ ,  $R = 0$ . For the Eckhaus curve (indicated by E)  $d = 0$  and  $\sigma_{1i} = 0$ . For the Hopf bifurcation curve (indicated by H)  $d \neq 0$  and  $\sigma_{1i} \neq 0$ . The secondary LR are stable within the shaded region. The dashed curve represents the linear stability curve.

number of eigenvalues was investigated for wave numbers in the range  $1.5 \leq \beta \leq 3.0$ . In order to determine the value of  $d$  for which the maximum growth rate of the leading eigenvalue,  $\sigma_{1r}$ , will occur, we fix the value of  $d$  to the one for which the maximum value of  $\sigma_{1r}$  was observed for a given value of  $b$ , and we then examine  $\sigma_{1r}$  as a function of  $b$ . For the Eckhaus curve at the zero growth rate point ( $\sigma_{1r} = 0$ ) we observed that  $\sigma_{1i} = 0$ . Our calculations have also shown that for  $d = 0$  maximum growth rate was observed when  $0.3 \leq b/\beta \leq 0.5$  (with a symmetric peak at  $0.5 \leq b/\beta \leq 0.7$ ). For the Hopf bifurcation curve at the zero growth rate point ( $\sigma_{1r} = 0$ ) we observed that  $\sigma_{1i} \neq 0$  and therefore a Hopf bifurcation takes place. This occurrence combined with the underlying two-dimensional steady solution shows that a bifurcation to a spatially periodic tertiary flow appears.

## 6. Concluding remarks

In this work we presented stability analysis of flows in an inclined channel uniformly heated without the imposition of a constant pressure gradient. Linear stability analysis for  $Pr = 7$ ,  $R = 0$  showed that our basic flow becomes unstable to LR disturbances for  $\gamma = 60^\circ$ , [2]. Next, non-linear secondary LR type equilibrium states were obtained numerically with the aid of the Chebyshev collocation point method and the Newton–Raphson iterative method for the same value of  $\gamma$ . We identified that these secondary equilibrium states bifurcate supercritically from the basic state. Non-linear properties of the secondary flow, such as the total mean flow, were also presented. Finally we studied the stability of the secondary flow, by applying the Floquet theory. We superimposed the general type of three-dimensional perturbations on the secondary equilibrium states. Traces of the Eckhaus and Hopf bifurcation curves were identified and our calculations showed that transition to a periodic tertiary flow can occur depending on the values of the parameters  $d$ ,  $b$ . The extension of the current work to include various values of the angle of inclination is currently under way and will be reported separately.

## References

- [1] M. Nagata, S. Generalis, Transition in convective flows heated internally, *J. Heat Trans. T. ASME* 124 (2002) 635–642.
- [2] S. Generalis, M. Nagata, Transition in homogeneously heated inclined plane-parallel shear flows, *J. Heat Trans. T. ASME* 125 (2003) 795–803.
- [3] S. Generalis, M. Nagata, Transition in internally heated shear flows in a vertical channel, *heat transfer in unsteady and transitional flows, Eurotherm 74* (2003) 117–122.
- [4] A. Kljenak, I. Horvat, J. Marn, Two-dimensional large-eddy simulation of turbulent natural convection due to internal heat generation, *Int. J. Heat Mass Trans.* 44 (2001) 3985–3995.
- [5] U. Ehrenstein, W. Koch, Three-dimensional wavelike equilibrium states in plane Poiseuille flow, *J. Fluid Mech.* 228 (1991) 111–148.